

# Blockwise Phase Rotation-Aided Analog Transmit Beamforming for 5G mmWave Systems

Md. Abdul Latif Sarker, Igbafe Orikumhi, Dong Seog Han and Sunwoo Kim

**Abstract**—In this letter, we propose a blockwise phase rotation-aided analog transmit beamforming (BPR-ATB) scheme to improve the spectral efficiency and the bit-error-rate (BER) performance in millimeter wave (mmWave) communication systems. Due to the erroneous construction of the conventional transmit beamforming, we design the BPR-ATB for achieving an efficient beam pattern and improving the Euclidean distance. To verify the effectiveness of the proposed BPR-ATB scheme, we employ an Alamouti coding technique at the transmitter and evaluate the bit-error-rate performance for a mmWave multiple-input and single-output system. The simulation results show that the proposed BPR-ATB scheme outperforms the conventional discrete Fourier transform-based ATB scheme.

**Index Terms**—5G-millimeter-wave systems, blockwise phase rotation, Alamouti coding, spectral, and BER performance.

## I. INTRODUCTION

THE millimeter-wave (mmWave) technology plays a major role in the fifth-generation (5G) wireless communications owing to the large bandwidth [1] and spectral efficiency [2]–[4]. The mmWave technology operates in the 30 to 300 GHz band [1], hence the large spectral resource in contrast with microwave technologies operating in the sub 6 GHz band [5]. Typically, mmWave system requires massive antenna arrays, which are equipped with the base station (BS) for achieving a highly directive beamforming [6]. For deployment of this system, the leading barriers are the hardware limitations, the channel sparsity, the free-space path loss, beamforming construction, and phase angle optimization.

The sparse nature of the channel and the discrete Fourier transform-based analog beamforming (DFT-ATB) schemes have been investigated in [2], [4], [6]–[10]. The authors designed a joint antenna selection based transmit beamforming in [8]. A phase control DFT based hybrid precoding scheme is presented in [9], [10]. Particularly, the traditional analog beamforming incurs a quantization error in communication systems owing to their subspace packing problem [5], [9], [11]. To get a better chordal distance of analog precoding, the authors proposed a Golden-Hadamard (GH) based precoding in [12]. Although the GH scheme achieved a remarkable bit-error-rate (BER) performance in microwave systems, the scheme shows a ‘beam squint’ challenge in highly directive systems. The ‘beam squint’ leads a higher channel spreading

factor due to the constructional leakage of the conventional analog beamforming [7]. Hence, we revise the results of [12, eq. (9)] and extend it to design a block phase rotation-aided analog transmit beamforming (BPR-ATB) for mmWave communication systems.

In this article, we propose a BPR-ATB scheme to obtain an efficient beam pattern and mitigate phase angle optimization challenges of traditional analog beamforming such as the DFT-ATB scheme. To this end, we seek to minimize the rotated beamwidth and enhance the Euclidean distance. We first revise the result of [12, eq. (9)] and design a BPR-ATB scheme to produce an efficient beam pattern and get a satisfactory spectral efficiency of the mmWave communications. We then implement the proposed BPR-ATB scheme with Alamouti code and set a parameter  $\kappa$  in the BER performance metric. We finally show the superiority of the proposed BPR-AB scheme over the DFT-ATB scheme in terms of a downlink mmWave multiple-input and single-output (MISO) systems through computer simulations.

## II. CHANNEL AND SIGNAL MODELS

We consider a downlink mmWave MISO system with  $N_t$  transmit antennas and a single antenna receiver ( $N_t \gg 1$ ). Then the received signal vector  $\mathbf{y} \in \mathbb{C}^{1 \times T}$  can be modeled as

$$\mathbf{y} = \sqrt{P}\mathbf{h}^H \mathbf{X} + \mathbf{z}, \quad (1)$$

where  $P$  denotes the transmit power,  $\mathbf{X}$  is the  $N_t \times T$  space-time codeword matrix,  $T$  is the number of time slot, and  $\mathbf{z} \sim \mathcal{CN}(0, \sigma^2)$  is additive white Gaussian noise vector with zero-mean. The narrow-band mmWave channel  $\mathbf{h} \in \mathbb{C}^{N_t \times 1}$  with  $L$  propagation paths [6], [8], that is

$$\mathbf{h} = \sqrt{\frac{N_t}{L}} \sum_l \alpha_l \mathbf{a}(\theta_l), \quad (2)$$

where  $\alpha_l$  is the complex gain of the  $l$ -th path,  $\theta_l$  represents the angle of departure of the  $l$ -th path,  $\mathbf{a}(\theta_l)$  denotes the transmit steering vector of the  $l$ -th path, which is given by

$$\mathbf{a}(\theta_l) = [1, e^{j\frac{2\pi d}{\lambda} \sin \theta_l}, \dots, e^{j\frac{(N_t-1)\pi d}{\lambda} \sin \theta_l}]^T, \quad (3)$$

the wavelength,  $\lambda = c/f_c$ ,  $c$  is the speed of light,  $f_c$  is the carrier frequency, and  $d = c/2f_c$  is the antenna spacing.

## III. BLOCKWISE PHASE ROTATION-AIDED ANALOG TRANSMIT BEAMFORMING DESIGN

Due to the ‘beam squint’ issue in the high dimensional ATB scheme, we first revise the result of [12, eq.(9)] in this section and then we extend to design a BPR-ATB scheme. Let the number of total transmit antennas  $N_t = 2^q$  and the revised geometrical number of antenna values  $\xi_{rev} = 0.2360 + \xi$ , where

This work was supported by Institute for Information & communications Technology Promotion(IITP) grant funded by the Korea government (MSIT: 2016-0-00208, High Accurate Positioning Enabled MIMO Transmission and Network Technologies for Next 5G-V2X Services) (corresponding author: Sunwoo Kim)

M. A. L. Sarker, I. Orikumhi and S. Kim are with the Department of Electronics and Computer Engineering, Hanyang University, Seoul 04763, South Korea. (e-mail: abdull123@hanyang.ac.kr; oigbaf2@hanyang.ac.kr; remero@hanyang.ac.kr).

D. S. Han are with the School of Electronics Engineering, Kyungpook National University, Daegu 41566, South Korea (e-mail: dshan@knu.ac.kr).

$\xi$  denotes the geometrically designed number of antennas [12]. Consider the space-time codeword matrix  $\mathbf{X}$  as

$$\mathbf{X} = \mathbf{F}_{2^q} \mathbf{S}, \quad (4)$$

where  $\mathbf{S}$  is a  $2^{q-1} \times T$  orthogonal space time block code matrix,  $\mathbf{F}_{2^q}$  be a  $2^q \times 2^{q-1}$  analog transmit beamforming matrix constructed by  $2^{q-1}$  columns of the revised  $2^q \times 2^q$  recursive Golden-Hadamard with block-diagonal matrices as follows

$$\mathbf{F}_{2^q} = \frac{1.6180}{\sqrt{\xi_{rev}}} \begin{bmatrix} \mathbf{W}_{2^{q-1}} & \mathbf{W}_{2^{q-1}} \\ \mathbf{W}_{2^{q-1}} & -\mathbf{W}_{2^{q-1}} \end{bmatrix} \mathbf{D}_{2^q}, \quad (5)$$

where  $\mathbf{W}_{2^{q-1}}$  is a  $2^{q-1} \times 2^{q-1}$  block Hadamard matrix,  $\mathbf{D}_{2^q}$  is a  $2^q \times 2^q$  block-diagonal matrix given as

$$\mathbf{D}_{2^q} = \begin{bmatrix} \mathbf{A}_{2^{q-1}} & \mathbf{B}_{2^{q-1}} \\ \mathbf{B}_{2^{q-1}} & -\mathbf{A}_{2^{q-1}} \end{bmatrix}, \quad (6)$$

$\mathbf{A}_{2^{q-1}}$  and  $\mathbf{B}_{2^{q-1}}$  are the  $2^{q-1} \times 2^{q-1}$  block-diagonal rotation matrix. By substituting (4) in (1), the system can achieve a spectral efficiency for MISO system given as

$$R = \log_2 \left\{ 1 + \frac{P}{\sigma^2} \mathbf{h}^H \mathbf{F}_{2^q} \mathbf{F}_{2^q}^H \mathbf{h} \right\}. \quad (7)$$

Particularly, the phase rotation on the transmitted signals is effectively equivalent to rotating the phases of the corresponding channel coefficients. It should be noted that, the conventional DFT-ATB scheme generates a satisfactory array gain with equivalent channel [8], [9], but this scheme suffers a phase angle optimization problem, which leads to a wide beam as shown in Fig. 1.

Let  $h_\nu$  be the  $\nu$ -th element of  $\mathbf{h}$  and  $\mathbf{f} \in \mathcal{F}$  be the effective analog beamforming vector. Thus, the DFT-ATB

based schemes can be formulated with the following optimal phase angle as

$$\begin{aligned} \varphi_\nu^{opt} &= \arg \max_{\varphi_\nu} \left| \sum_{\nu=1}^{N_t} h_\nu^* \mathbf{f}(\varphi_\nu) \right| \\ \text{s.t. } \varphi_\nu &\in \left\{ \frac{2\pi b}{2^B} \middle| b = 0, 1, \dots, 2^B - 1 \right\}, \\ \text{and } \nu &= 1, \dots, N_t. \end{aligned} \quad (8)$$

We see in (8) and in Fig.1 that the conventional DFT-ATB scheme generates an extensive beamspace with a mmWave channel, which contains a wide phase angle. As a result, the user suffers from a high computational burden to optimize the traditional beam pattern.

To address the phase angle optimization problem, we reformulate (8) as follows: Let  $\varphi_\nu \in \{\phi_{\nu_1}, \psi_{\nu_2}\}$ , where  $\phi_{\nu_1}$  and  $\psi_{\nu_2}$  are the block phase angle of  $\mathbf{A}_{2^{q-1}}$  and  $\mathbf{B}_{2^{q-1}}$ . We set  $\phi_{\nu_1}$  and  $\psi_{\nu_2}$  in the designed transmit beamformer of  $\mathbf{F}_{2^q}$ . Then the optimal block phase angle is given by

$$\begin{aligned} (\phi_{\nu_1}^{opt}, \psi_{\nu_2}^{opt}) &= \arg \max_{\phi_{\nu_1}, \psi_{\nu_2}} \left| \sum_{\nu_1=1}^{2^{q-1}} \Omega_{\nu_1} + \sum_{\nu_2=1}^{2^{q-1}} \Omega_{\nu_2} \right| \\ \text{s.t. } \phi_{\nu_1} &\in \left\{ \frac{2\pi b_1}{2^{q-1}} \middle| b_1 = 0, 1, \dots, 2^{q-1} - 1 \right\}, \\ \psi_{\nu_2} &\in \left\{ \frac{2\pi b_2}{2^{q-1}} \middle| b_2 = 2^{q-1}, \dots, 2^q - 1 \right\}, \\ \text{and } \nu_1 = \nu_2 &= 1, \dots, 2^{q-1}, \end{aligned} \quad (9)$$

where  $\Omega_{\nu_1} = h_{\nu_1}^* \mathbf{f}_{\nu_1}(\phi_{\nu_1})$ ,  $\Omega_{\nu_2} = h_{\nu_2}^* \mathbf{f}_{\nu_2}(\psi_{\nu_2})$ ,  $\mathbf{f}_{\nu_1}(\phi_{\nu_1}) = e^{j\phi_{\nu_1}} / \sqrt{2^{q-1}}$ , and  $\mathbf{f}_{\nu_2}(\psi_{\nu_2}) = e^{j\psi_{\nu_2}} / \sqrt{2^{q-1}}$ . Consider  $\mathcal{C} \in \{\mathcal{C}_{\nu_1}, \mathcal{C}_{\nu_2}\}$  as the set of indexes of useful antennas, where  $\mathcal{C}_{\nu_1}$  and  $\mathcal{C}_{\nu_2}$  are the subset of  $\mathcal{C}$ . Using (9), we demonstrate the proposed BPR-ATB scheme in **Algorithm 1**. We see in **Algorithm 1**, the designed transmit beamformer leads to an optimal block phase angle, which overcome the phase angle

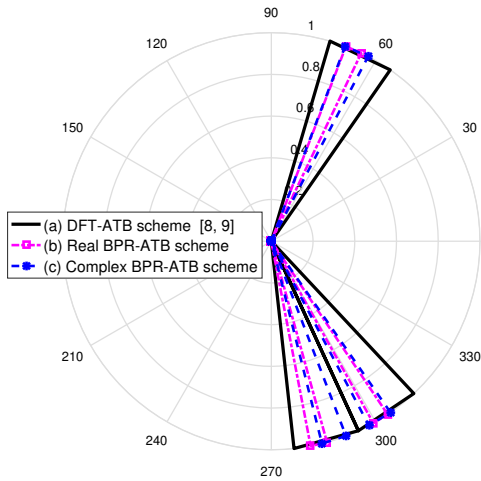


Fig. 1. The rose diagram of beam pattern: (a) the effective equivalent mmWave channel with the conventional DFT-ATB scheme [8], [9] in solid lines, (b) and (c) the effective equivalent mmWave channel with the proposed BPR-ATB scheme in dotted lines.

---

#### Algorithm 1 Proposed BPR-ATB based Algorithm

---

- 1: **Input parameters:**  $\mathbf{h}, q$
  - 2: **Output:**  $\mathbf{f}_{2^q}^{opt}$
  - 3: Find  $\varphi_\nu^{opt} = \{\phi_{\nu_1}^{opt}, \psi_{\nu_2}^{opt}\}$  and  $\Omega_\nu = \{\Omega_{\nu_1}, \Omega_{\nu_2}\}$
  - 4: **Begin**  $\mathcal{C} \in \{\mathcal{C}_{\nu_1}, \mathcal{C}_{\nu_2}\}$ ,  $\nu_1 = \nu_2$
  - 5: **for**  $\nu_1 = 1 : 2^{q-1}$  **do**
  - 6: Obtain  $\nu_1^{opt} = \arg \max_{\nu_1 \in \mathcal{C}_{\nu_1}} |\Omega_{\nu_1}|$ .
  - 7: **end**
  - 8: **for**  $\nu_2 = 1 : 2^{q-1}$  **do**
  - 9: Obtain  $\nu_2^{opt} = \arg \max_{\nu_2 \in \mathcal{C}_{\nu_2}} |\Omega_{\nu_2}|$ .
  - 10:  $\mathcal{C} := \nu_1^{opt} \cup \nu_2^{opt}$ .
  - 11:  $\mathcal{C} := \mathcal{C} \bmod \{\nu_1^{opt}, \nu_2^{opt}\}$ .
  - 12: **end for**
  - 13: Obtain  $\mathbf{f}_{2^q}^{opt} = (e^{j\phi_{\nu_1}} + e^{j\psi_{\nu_2}}) / \sqrt{2^{q-1}}$  according to (9).
-

TABLE I  
DIFFERENT POWER FACTOR OF RF PRECODING

Power factor of RF precoding, $\kappa =  \mathbf{F}_{i,j} ^2$			
DFT[5, 9]	HA [14]	BPR	
		Real case	Complex case
$\frac{1}{N_t}$	$\frac{1}{N_t}$	$\frac{(1 + \sqrt{5})^2}{4\xi_{rev}}$	$\frac{(j + \sqrt{3})^2}{4\xi_{rev}}$

optimization issue of (8) and effortlessly performs well with the fifth-generation wireless channel.

#### IV. SIMULATION RESULTS AND DISCUSSION

In this section, we compare the proposed BPR-ATB scheme against the conventional DFT-ATB scheme via computer simulations. To show the superiority of the proposed scheme, we employ a complex Alamouti coding technique at the transmitter. For example, if we use the  $k$ -th entry of a complex alamouti code with time slot  $T = 2$  in (4), then the codeword matrix  $\mathbf{X}$  is given by

$$\begin{aligned} \mathbf{X} &= \sqrt{\gamma_0 \kappa} \mathbf{F} \mathbf{S}_k \\ &= \sqrt{\gamma_0 \kappa} \mathbf{F} \begin{bmatrix} s_{11} & -s_{21}^* \\ s_{21} & s_{11}^* \end{bmatrix}, \end{aligned} \quad (10)$$

where  $\mathbf{S}_k$  is the  $k$ -th entry of  $2 \times 2$  complex Alamouti code [13], symbols  $s_{11}$  and  $s_{21}$  belongs to a quadrature amplitude modulation (QAM) constellation,  $\kappa = |\mathbf{F}_{i,j}|^2$  is a power factor of the  $(i, j)$  element of analog beamforming  $\mathbf{F}$ , and  $\gamma_0$  is the received signal-to-noise power (SNR). The  $\kappa$  value depends on the structure of  $\mathbf{F}$  matrix (see in Table I).

Consider  $\mathbf{S}_k$  and  $\mathbf{S}_l$  as the transmitted and decoded space-time codewords, respectively, where  $k \neq l$ . The union bound on the bit-error-rate (BER) is formulated as [15]

$$BER \leq \sum_{k \neq l} \frac{e(\mathbf{S}_k, \mathbf{S}_l)}{\log_2(M)} Q\left(\Xi_{k,l} \sqrt{\frac{\gamma_0 \kappa}{2}}\right), \quad (11)$$

where  $M$  denotes the constellation size, the operator  $Q(\cdot)$  represents the Q-function [15],  $\Xi_{k,l} = \|\mathbf{h}_{eq}^H \mathbf{e}_{k,l}\|_F$  where the operator  $\|\cdot\|_F$  denotes a Frobenius norm,  $\mathbf{e}_{k,l}$  represents an error matrix between the codewords  $\mathbf{S}_k$  and  $\mathbf{S}_l$ ,  $e(\mathbf{S}_k, \mathbf{S}_l)$  is the Hamming distance between the bit mappings corresponding to the vectors  $\mathbf{S}_k$  and  $\mathbf{S}_l$ . Invoking the Chernoff upper bound  $Q(x) \leq e^{-x^2/2}$  in (11), the pairwise error probability can be upper bounded with an equivalent channel  $\mathbf{h}_{eq}$  as

$$P_r(\mathbf{S}_k \rightarrow \mathbf{S}_l | \mathbf{h}_{eq}) \leq e^{-\frac{\gamma_0 \kappa \Xi_{k,l}^2}{4}}, \quad (12)$$

where  $\mathbf{h}_{eq} = \mathbf{F}^H \mathbf{h}$ , and  $\Xi_{k,l}^2$  can be expressed as

$$\Xi_{k,l}^2 = \text{tr}[\mathbf{h}_{eq}^H \mathbf{R}_{k,l} \mathbf{h}_{eq}]. \quad (13)$$

The property of the error matrix  $\mathbf{R}_{k,l} = \mathbf{e}_{k,l} \mathbf{e}_{k,l}^H = a \mathbf{I}$  for the orthogonal space-time block coding,  $a$  is a constant depending on the constellation [see in APPENDIX A].

Throughout the simulations, we assumed the parameters of Table II with different  $\kappa$  factor of Table I. We measure and set the parameter  $\kappa$  in the simulations such as  $\kappa = 0.25$  for both the DFT-ATB scheme [5] and the Hadamard based

TABLE II  
SIMULATION PARAMETERS

Total number of transmit antennas	$N_t = 4$
Total number of receive antenna	$N_r = 1$
Selected number of RF Chains	$N_{RF} = 2$
Channel path	$L = 3$
SNR	$\gamma_0 = 20$ dB
Carrier frequency	$f_c = 60$ GHz
Wavelength	$\lambda = 5$ mm
Antenna spacing distance	$d = \lambda/2$
Modulation scheme	64 QAM

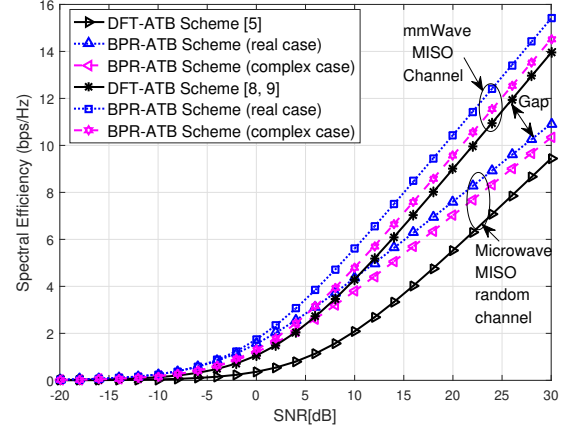


Fig. 2. Spectral Efficiency versus SNR ( $N_t = 4, N_{RF} = T = 2$ , and  $N_r = 1$  with different  $\kappa$  values of the analog transmit beamforming.

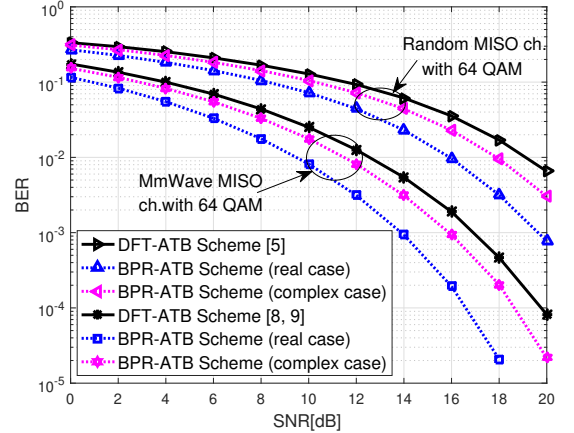


Fig. 3. BER performance of 64QAM modulated Alamouti coding with different  $\kappa$  values of analog transmit beamforming.

ATB scheme [14],  $\kappa = 0.50$  for the proposed real BRP-ATB scheme, and  $\kappa = 0.31$  for the proposed complex BRP-ATB scheme while  $q = 2$  and  $N_t = 4$  is applied in Table I.

Fig. 2 illustrates the spectral efficiency comparisons of the proposed BPR-ATB scheme against the conventional DFT-ATB scheme. For the mmWave setup, the performance of the spectral efficiency is around 1.8 bits/s/Hz at 30 dB SNR values. The proposed BPR-ATB scheme also achieved good spectral performance with the traditional MISO random channel environment as shown in Fig. 2.

Fig. 3 shows the BER performance of the  $4 \times 2$  BPR-

ATB scheme using  $2 \times 2$  Alamouti coding and 64QAM constellations. We see that the DFT-ATB scheme achieves a worse spectral efficiency and BER performance in [5], [8], [9] for both mmWave and the familiar microwave MISO systems owing to their wide beam pattern (see in Fig.1) and a teeny  $\kappa$  factor (see in Table I). The proposed BPR-ATB scheme provides at least 2 dB more BER performance with the DFT-ATB scheme. Furthermore, both spectral efficiency and BER performance of a complex case of the proposed BPR-ATB scheme is slightly worsened than that of a real case of the proposed BPR-ATB scheme because of the reduction of the value of the Golden ratio.

## V. CONCLUSIONS

We proposed a BPR-ATB scheme to achieve an efficient beam pattern for the mmWave systems. We verify the effectiveness of the proposed BPR-ATB scheme by computer simulation and compare the performance with the conventional DFT-ATB scheme. The traditional DFT-ATB scheme exhibited a worse spectral efficiency about 1.8 bits/s/Hz and BER performance difference of 2 dB when compared with the proposed BPR-ATB scheme. Lastly, the proposed BPR-ATB scheme can be extended further to the next generation multiple-input and multiple-output non-orthogonal multiple-access (MIMO-NOMA) systems, which will be explored in future studies.

## APPENDIX A

From (11), we can measure as a general single-input and single-output case of BER as follows:

$$\begin{aligned} P_{e,b} &= \int_0^\infty Q(a\sqrt{\gamma}) p_\gamma(\gamma) d\gamma \\ &= \frac{1}{\pi} \int_0^{\frac{\pi}{2}} \mathcal{M}_\gamma \left( \frac{-a^2}{2\sin^2\theta} \right) d\theta \end{aligned} \quad (14)$$

where  $\gamma = \kappa\gamma_0/2$ . The Gaussian Q-fuction  $Q(x)$  is given by [15]

$$Q(x) = \frac{1}{\pi} \int_0^{\frac{\pi}{2}} \exp \left( \frac{-x^2}{2\sin^2\theta} \right) d\theta. \quad (15)$$

It is noted that in (14),  $\mathcal{M}_X(-s) = \int_0^\infty e^{-sx} p_X(x) dx$  is a moment generating function (MGF) of random variable  $X$  where  $\mathcal{M}_\gamma(s) = \int_0^\infty e^{s\gamma} p_\gamma(\gamma) d\gamma$  is the Laplace transform of  $p_\gamma(\gamma)$  with the exponent reversed sign. By using the Rayleigh channel, we can consider  $p_\gamma(\gamma) = \exp(-\gamma/\bar{\gamma})/\bar{\gamma}$ , where  $\gamma \geq 0$  and  $\bar{\gamma}$  idenotes the average SNR per bit. Hence, the Laplace transform is given by

$$\mathcal{M}_X(-s) = \frac{1}{1+s\bar{\gamma}}, \quad s > 0. \quad (16)$$

Substituting (16) into (14) gives

$$P_{e,b}(a, \bar{\gamma}) = \frac{1}{2} - \frac{a}{2} \sqrt{\frac{\bar{\gamma}}{2+a^2\bar{\gamma}}}. \quad (17)$$

For the simplicity, (17) is derived for the binary phase shift keying (when  $a = 1$ ) modulation scheme, which can be straightforwardly extended to other modulation cases. For example, M-ary phase shift keying modulation scheme: we consider  $a^2 = 2\sin^2(\pi/M)$  and applying (16) in (14), then

we follow directly (17) and obtain the bit-error-rate probability for Rayleigh fading channel as

$$\begin{aligned} P_{e,b}(a, \bar{\gamma}, M) &= \frac{(M-1)}{M} - \frac{\sqrt{\mu}}{2} + \\ &\quad \frac{(M-1)\sqrt{\mu}}{M} \tan^{-1} \left( \sqrt{\mu} \cot \frac{\pi}{M} \right), \end{aligned} \quad (18)$$

where  $\mu = (\bar{\gamma} \sin^2 \frac{\pi}{M}) / (1 + \bar{\gamma} \sin^2 \frac{\pi}{M})$ . Similarly, using (14) and (16), we can measure the BER probability for M-ary QAM modulation as

$$\begin{aligned} P_{e,b}(a, \bar{\gamma}, M) &= \frac{4\zeta}{\pi} \int_0^{\frac{\pi}{2}} \left( 1 + \frac{3\bar{\gamma}}{2(M-1)\sin^2\theta} \right)^{-1} d\theta \\ &\quad - \frac{4\zeta^2}{\pi} \int_0^{\frac{\pi}{4}} \left( 1 + \frac{3\bar{\gamma}}{2(M-1)\sin^2\theta} \right)^{-1} d\theta, \end{aligned} \quad (19)$$

where  $a^2 = 3/(M-1)$  and  $\zeta = 1 - (1/\sqrt{M})$ .

## REFERENCES

- [1] Z. Pi and F. Khan, "An introduction to millimeter-wave mobile broadband systems," *IEEE Commun. Mag.*, vol. 49, no. 6, pp. 101–107, 2011.
- [2] J. Brady, N. Behdad, and A. M. Sayeed, "Beamspace mimo for millimeter-wave communications: System architecture, modeling, analysis, and measurements," *IEEE Trans. Antennas Propag.*, vol. 61, no. 7, pp. 3814–3827, 2013.
- [3] I. Ahmed, H. Khammari, A. Shahid, A. Musa, K. S. Kim, E. De Poorter, and I. Moerman, "A survey on hybrid beamforming techniques in 5g: Architecture and system model perspectives," *IEEE Commun. Surveys Tuts.*, vol. 20, no. 4, pp. 3060–3097, 2018.
- [4] M. A. L. Sarker, M. F. Kader, and D. S. Han, "Rate-loss mitigation for a millimeter-wave beamspace mimo lens antenna array system using a hybrid beam selection scheme," *IEEE Syst. J.*, vol. 14, no. 3, pp. 3582–3585, 2020.
- [5] D. J. Love and R. W. Heath, "Limited feedback unitary precoding for orthogonal space-time block codes," *IEEE Trans. Signal Process.*, vol. 53, no. 1, pp. 64–73, 2005.
- [6] R. W. Heath, N. González-Prelcic, S. Rangan, W. Roh, and A. M. Sayeed, "An overview of signal processing techniques for millimeter wave mimo systems," *IEEE J. Sel. Topics Signal Process.*, vol. 10, no. 3, pp. 436–453, 2016.
- [7] X. Gao, L. Dai, S. Zhou, A. M. Sayeed, and L. Hanzo, "Wideband beamspace channel estimation for millimeter-wave mimo systems relying on lens antenna arrays," *IEEE Trans. Signal Process.*, vol. 67, no. 18, pp. 4809–4824, 2019.
- [8] H. Li, Q. Liu, Z. Wang, and M. Li, "Transmit antenna selection and analog beamforming with low-resolution phase shifters in mmwave miso systems," *IEEE Commun. Lett.*, vol. 22, no. 9, pp. 1878–1881, 2018.
- [9] L. Liang, W. Xu, and X. Dong, "Low-complexity hybrid precoding in massive multiuser mimo systems," *IEEE Wireless Commun. Lett.*, vol. 3, no. 6, pp. 653–656, 2014.
- [10] K. Satyanarayana, M. El-Hajjar, P. Kuo, A. Mourad, and L. Hanzo, "Hybrid beamforming design for full-duplex millimeter wave communication," *IEEE Trans. Veh. Technol.*, vol. 68, no. 2, pp. 1394–1404, 2019.
- [11] H. Wang, Y. Li, X. Xia, and S. Liu, "Unitary and non-unitary precoders for a limited feedback precoded ostbc system," *IEEE Trans. Veh. Technol.*, vol. 62, no. 4, pp. 1646–1654, 2013.
- [12] M. A. L. Sarker, M. F. Kader, M. H. Lee, and D. S. Han, "Distortion-free golden-hadamard codebook design for miso systems," *IEEE Commun. Lett.*, vol. 22, no. 10, pp. 2152–2155, 2018.
- [13] S. M. Alamouti, "A simple transmit diversity technique for wireless communications," *IEEE J. Sel. Areas Commun.*, vol. 16, no. 8, pp. 1451–1458, 1998.
- [14] S. Kundu, D. A. Pados, W. Su, and R. Grover, "Toward a preferred 4 x 4 space-time block code: A performance-versus-complexity sweet spot with linear-filter decoding," *IEEE Trans. Commun.*, vol. 61, no. 5, pp. 1847–1855, 2013.
- [15] J. G. Proakis, *Digital Communications*. 4th ed. New York, NY, USA: McGraw-Hill, 2007.